www.cadanda.com
Computer-Aided Design AND APPLICATIONS

A Prototype CAE Tool for Mechanical Optimization of Dental CAD/CAM Process for All-ceramic Restoration

Kyo Shindo[1], Laurent Tapie[2], Nicolas Schmitt[3] and Elsa Vennat[4]

[1]Laboratoire de Mécanique des Sols, Structures et Matériaux, CentraleSupélec, Université Paris-Saclay ; Unité de Recherches Biomatériaux Innovants et Interfaces, Université de Paris, Université Sorbonne Paris Nord, kyo.shindo@protonmail.com
[2]Unité de Recherches Biomatériaux Innovants et Interfaces, Université de Paris, Université Sorbonne Paris Nord, laurent.tapie@univ-paris13.fr
[3]Laboratoire de Mécanique et Technologie, ENS Paris-Saclay, Université Paris-Saclay ; Université Paris-Est-Créteil, nicolas.schmitt@ens-paris-saclay.fr
[4]Laboratoire de Mécanique des Sols, Structures et Matériaux, CentraleSupélec, Université Paris-Saclay ; Unité de Recherches Biomatériaux Innovants et Interfaces, Université de Paris, Université Sorbonne Paris Nord, elsa.vennat@centralesupelec.fr

Corresponding author: Kyo Shindo, kyo.shindo@protonmail.com

Abstract. Almost all of the world's population today has faced, are facing or will be facing a dental problem. When a lesion mildly affects the tooth, a bonded fixed partial denture can be proposed. Prosthesis design is currently performed based on geometrical considerations (dental preparation shape, surrounding teeth, for which geometry is acquired prior to design) and recommendations. Frequent prostheses mechanical failures are reported. Surprisingly, however, no mechanical consideration is included in the CAD/CAM process. In this paper, a CAE step in the prosthesis design workflow is proposed based on data that is already acquired and generated (available in the digital workflow). Based on a clinical case, the integration of a mechanical optimization step in the process with no additional handling by the dentist is presented, and its feasibility is proved. The proposed mechanical optimization induces a substantial overstress reduction in the prosthesis. This study paves the way towards the mechanical optimization of each prosthesis produced by CAD/CAM with no additional cost or practitioner training.

Keywords: dental CAD/CAM, patient-specific Bio-CAD, FEA mechanical optimization, dental CAE tool.
DOI: https://doi.org/10.14733/cadaps.2022.426-448

1 INTRODUCTION

Restorative dentistry encompasses the area of individual restoration of teeth employing metallic or non-metallic materials. This practice aims to rehabilitate the structural integrity of a decayed tooth by minimizing the loss of sound tissue. Several techniques exist, including the bonded fixed partial

denture technique, which consists of bonding a pre-fabricated all-ceramic prosthesis on the prepared tooth using an appropriate adhesive procedure.

Functional constraints need to be considered at the early stage of the design process of an all-ceramic dental restoration. An appropriate geometrical relationship between the prosthesis and the neighboring teeth is necessary to ensure a good occlusion, which is, in turn, essential for the mastication function [55]. Depending on the type of tooth, an appropriate shade is also required, given the importance of an aesthetic appearance the patient. Lastly, the restoration supports mechanical loads during the mastication process and must have a significant lifetime.

Chewing is a complex phenomenon allowing the reduction of the size of food to ingest it better. This physiological function involves significant mechanical effort; the masseter muscle used being one of the most powerful in the human body. The surfaces of loading used during a masticatory cycle are not constant, as the lower jaw can make a wide variety of movements thanks to the mobility of the temporomandibular joints [26]. Also, the intensity of mechanical loading is variable and depends on several factors, such as the texture of the food or the dental and muscular anatomy of the patient [6,22].

Due to these repeated loads, the durability of such restorations remains limited. Depending on the type of ceramic used, 4% to 9.3% of failures occur within the first five years of use [45]. Moreover, it is well-known that ceramic prostheses are prone to brittle fracture and still have a shorter lifetime than metallic restorations [17]. Consequently, improving their lifetime requires taking mechanical considerations into account in the current design method of all-ceramic restoration.

The design and fabrication processes of prosthetic parts have experienced significant developments during the last 30 years with the development of 3D digitization technologies with today's accessible cost for dental offices [4] and Computer-Aided Design (CAD) / Computer-Aided Manufacturing (CAM) process [33,38]. CAD/CAM allows designing and producing one all-ceramic dental restoration in a unique appointment with the dentist [9,24].

For now, the CAD design of the dental prosthetic restoration is only constrained by aesthetic and geometrical considerations [1]. The patient-specific anatomical data are digitized and used along with reference to tooth geometries selected in databases to create a 3D model of the future restoration (Figure 1) [51]. Typically, the restoration design protocol is based on an appropriate reconstruction of the prepared tooth. The design of the inner shape should fit the tooth prepared by the dentist to be bonded on the remaining dental tissues. The design of the outer shape might fit the neighboring situation (contacts with adjacent and opposite teeth) [48].

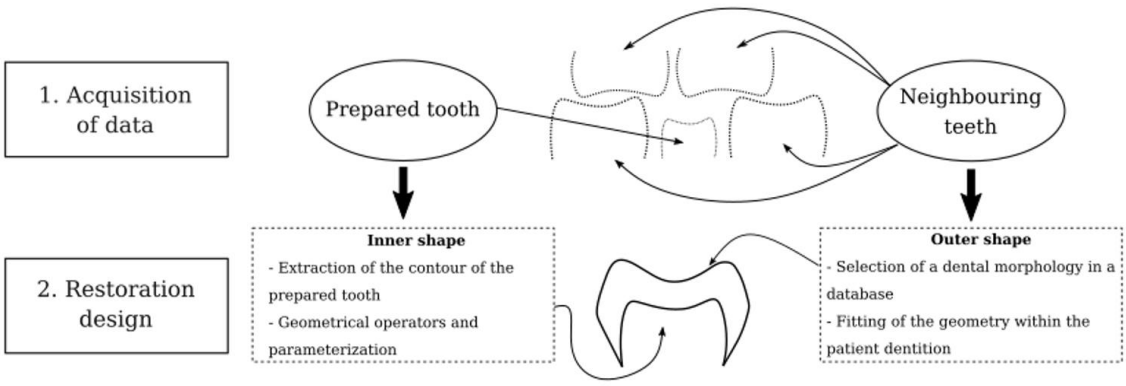

Figure 1: Standard dental computer-aided design (CAD) process guidelines.

For the design of the outer shape, parameterized geometrical models of dental crown morphology are provided within dental CAD software [51]. Geometrical tools (positioning, scaling, morphing) are used to adapt the parameterized CAD model of the tooth to the clinical case [60]. The algorithm used and the automation level of the process vary from one software to another. The design of the inner shape is based on the prepared tooth surface that will be bonded to the restoration. Depending on the CAD software algorithm, parametric transformations (homothetic or offsetting) are applied to that surface in order to introduce an appropriate gap between the prosthetic inner shape and the tooth [50,61]. Following the design phase, tool paths are calculated and transmitted to a CNC milling machine [15,28].

No specific Computer-Aided Engineering (CAE) tool is associated with dental CAD software to account for mechanical constraints in the design task. In the classical dental CAD/CAM process, warnings are mainly based on geometrical constraints, e.g., the prosthesis local thickness is above a minimum value. This limit is related to material machining constraint: a minimal milled thickness of material without chipping; a warning that the designer can overcome. Thus, mechanical considerations are mostly linked with the dentist or dental technician's expertise. Consequently, significant improvement may be expected by integrating a robust mechanical CAE tool in the prosthesis design process to minimize the failure of future prosthetic restoration assemblies and extend their lifetime. In return, such improvement requires an accurate description of the mechanical behavior of materials and assemblies.

In-vivo, in-vitro and numerical studies have already been undertaken to understand the mechanical behavior of all-ceramic restorations. Finite element analyses in dentistry have permitted to estimate the stress field and localize the zones of stress concentration inside an all-ceramic dental restoration [30,39]. For crown prostheses, Bowley and al. and Maghami et al. have shown that tensile stresses occur at the junction with the adhesive layer [2,32]. As brittle materials are sensitive to such stresses, those areas act like vulnerable zones within the structure [7,11,25,53]. Clinical observations using optical fractography confirm that most of the failures of all-ceramic prostheses initiate close to the prosthesis's inner surface [20,41,47,52]. Moreover, Sornsuwan & Swain, Zhang et al. and Miura et al. have shown on a simplified axisymmetric model of a restored tooth that the inner shape geometry significantly influences the prosthetic restoration's mechanical strength [36,49,59]. Both experimental and numerical studies reveal that the increase in ceramic thickness beneath the loading area reduces the bi-axial tensile stresses located at the adhesive/ceramic junction.

Nevertheless, such results are difficult to translate into clinical practice. On the one hand, in-vivo studies are case reports by clinicians making it difficult to identify the leading design parameters. Moreover, their interdependency influences the prosthetic restoration assembly mechanical behavior. On the other hand, in-vitro and numerical studies results are not accessible to dental practitioners, who are not specialists in mechanical science. Therefore, they encountered difficulties translating the experimental or numerical results into clinical guidelines or adapting such results to a patient-specific case.

To overcome the mentioned difficulties and integrate mechanical constraints during the CAD process, this article presents an additional Computer-Aided Engineering (CAE) method and tool for the design process of dental crowns (i.e., a restoration covering the coronary part of teeth). Design data embedded in current dental CAD/CAM systems are used to optimize the prosthesis shape with a high level of automation. In addition, in response to in-vitro and in-vivo studies underlying the weakness of dental prostheses, a methodology is proposed to optimize the design of the inner shape of restorations by locally reducing the developed tensile stresses. The CAE tool and associated methodology are tested on a real tooth restoration case.

2 PROSTHESIS COMPUTER-AIDED ENGINEERING TOOL

The proposed additional CAE analysis occurs after an initial design process with classical CAD/CAM software. It uses the CAD models of the prosthesis and of the dental environment (Figure 2). First,

a geometrical CAD model of the restored tooth composed of three parts (prosthesis, joint adhesive layer, and dental preparation) is created using an appropriate reverse-engineering algorithm and CAD operations (section 2.2). Then, a preliminary finite element analysis (FEA) model is subsequently created from a mechanical description specific to the clinical case. It makes it possible to locate the weakest points in the different parts of the assembly (section 2.3). Associated with an optimization procedure, the prosthesis geometry is locally adapted to reduce the stresses to a more sustainable level (section 2.5).

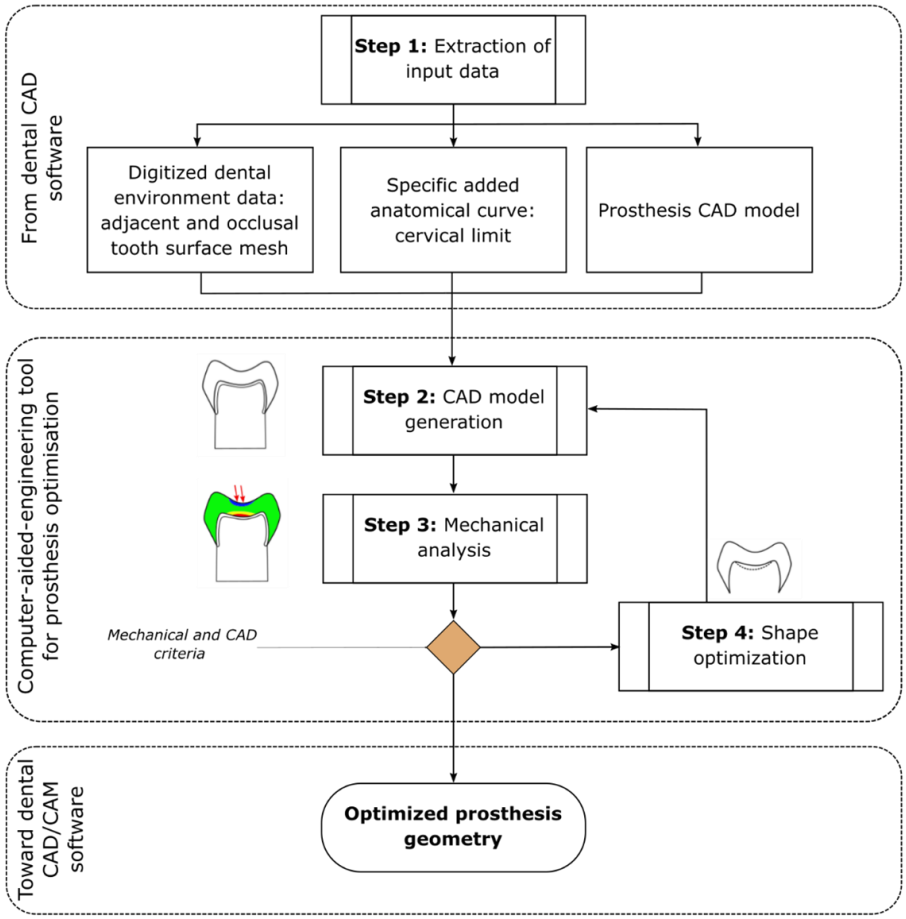

Figure 2: Proposed CAE structure for dental CAD/CAM processing.

The CAD methods and algorithms chosen to build the CAE enriched CAD/CAM process are all selected and aggregated to be fully automatable for dental practitioners considering an easy implementation in technical solutions.

2.1 Step 1: Extraction of Input Data

The input data are extracted from a dental CAD software. Data are those used to design the prosthesis, as explained in detail in Figure 1:

- Digitized dental environment data: during the digitization process, two surface meshes representing (1) the tooth to be restored and its adjacent teeth, (2) the opposite teeth

that will be in contact with the future prosthesis. These point cloud data are mostly stored in STL or PLY file format. According to recent work, the most efficient cameras can achieve a precision of less than 10 µm [12,51].

- Specifically added anatomical curve: during the CAD process, the designer plots the contour of the prepared tooth on the corresponding mesh, called cervical limit. This contour corresponds to the boundary between the remaining tooth tissue and those milled by the dental practitioner. The curve is mostly modeled with a B-spline.
- Prosthesis initial surface CAD model: as previously explained, the prosthesis shape is obtained by the junction of its inner and outer shapes. Surface mesh model are described in STL or PLY format, or parametric model, such as B-Spline, NURBS or Hermite polynomials.

2.2 Step 2: CAD Model Generation

The complete CAD model of the restored tooth assembly has to be designed in order to perform a patient-specific finite element analysis. To define the three material domains and generate the initial 3D FE mesh, closed shapes of each part of the restoration assembly are modeled from the geometrical models available:

- the prepared tooth shape is described with a surface boundary open mesh model,
- the prosthesis shape is described with a surface boundary closed mesh model or closed parametric model,
- the adhesive layer which is not a part of the initial CAD model; this free volume is associated to a set of dimensional parameters representing the adhesive thicknesses in specific location. It is created between the prepared tooth shape, the cervical limit and the inner shape of the prosthesis.

Then to each domain, constitutive equations are associated to describe the mechanical behavior of the constitutive material. In the proposed CAE method, the three parts' models are created using Nonuniform rational B-spline surfaces (NURBS) (Figure 3). NURBS models are commonly adopted as they allow modeling complex shapes like those encountered in dental CAD [14,44]. NURBS model can be associated with mesh points clouds such as those experienced in dental CAD. From a digital workflow point of view, NURBS model can be embedded in STEP (STandard for the Exchange of Product model data) or IGES (Initial Graphics Exchange Specification) file formats that are interoperable with most of the FEA software.

In the proposed CAE method, the input data (extracted from the dental CAD software) are pre-processed with an algorithm to be converted in NURBS surfaces. Then they are processed with elementary CAD operations (cutting, extrusion, filling) to obtain a restoration assembly model with closed boundaries material domains.

2.2.1 Step 2.1: data preparation

Data preparation aims at isolating the prepared tooth geometry necessary to design the restoration assembly (Figure 4). The B-spline curve, representing cervical limit, extracted from the dental CAD software, is used to cut the mesh containing the prepared tooth to isolate the tooth preparation shape. After the cutting operation, a mesh of the isolated prepared tooth is created.

2.2.2 Step 2.2: NURBS model association

The mesh of the isolated prepared tooth, coming from step 2.1, and the mesh of the prosthesis shape coming from the dental CAD software, if applicable, are both associated with NURBS surfaces using a reverse-engineering algorithm (Figure 5). The topological and geometrical consistencies of the NURBS model have been established in several biomedical engineering applications such as medical devices design and finite element analysis or medical diagnosis [37].

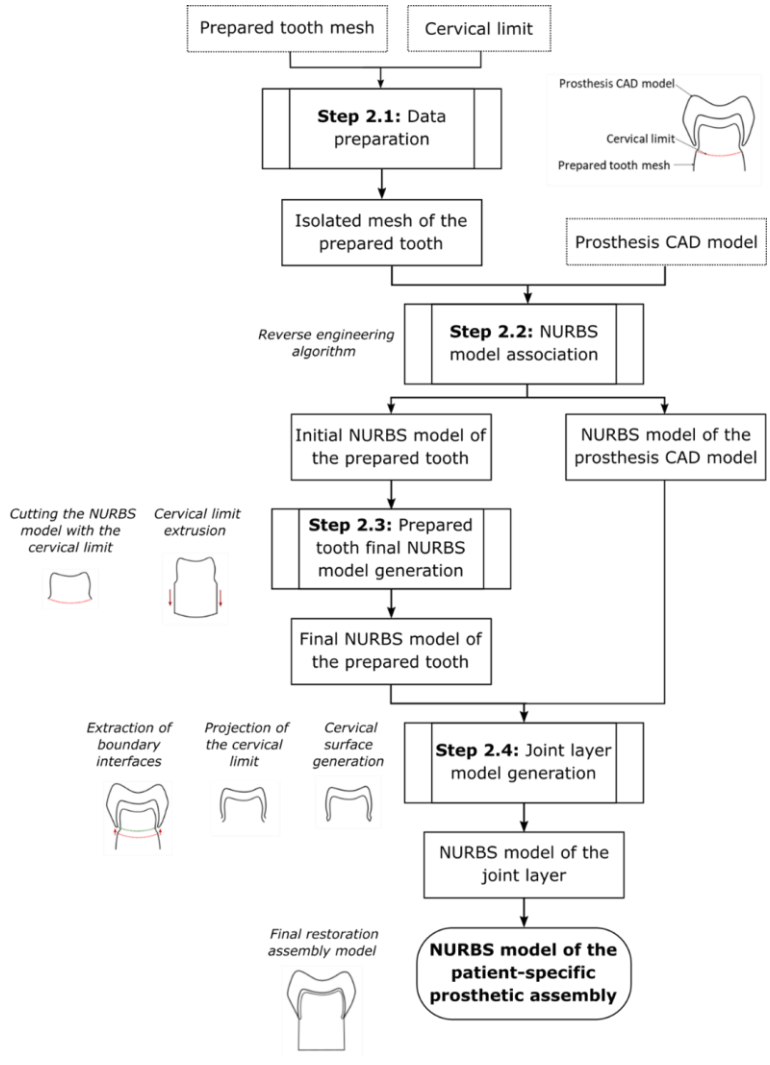

Figure 3: Patient specific geometrical model generation guidelines.

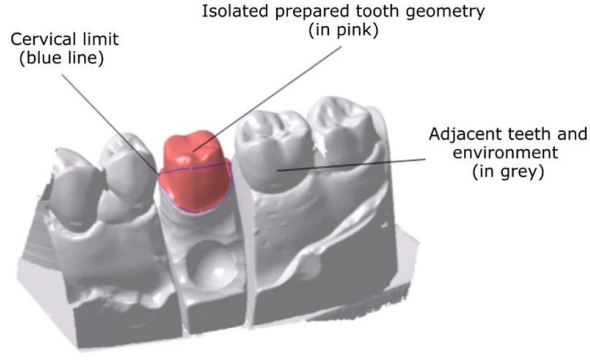

Figure 4: Digitized dental environment mesh data and associated specific anatomical curve.

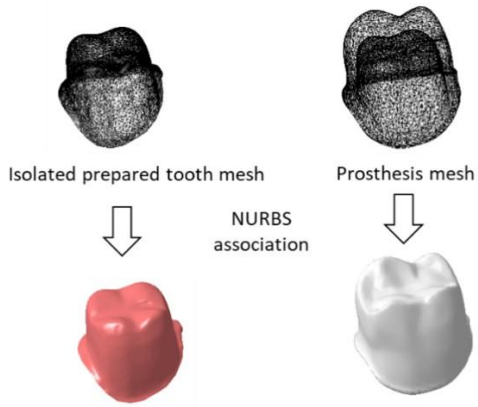

Figure 5: NURBS models association to dental CAD meshes.

Several surface reconstruction methods directly identify control points and their relative weight on a 3D point cloud [8,31,58]. However, these methods are time-consuming and have limited accuracy. In the developed CAE tool, Yoo et al.'s algorithm is implemented [57]. It is based on the interpolation of a smooth implicit surface, which is later used to compute a rectangular B-Spline curve net for the surface reconstruction. Several experimental results emphasize the robustness of this method to automatically and quickly associate B-Spline curve net to point clouds data from medical imaging or digitizing. A very small geometric tolerance can be obtained by adjusting the algorithm parameters. The algorithm has been implemented using Python 2.7 with Numpy and FreeCAD libraries [13,44].

2.2.3 Step 2.3: prepared tooth final model generation

To obtain the final NURBS model of the prepared tooth (Figure 6), a root-like surface is generated by extrusion of the cervical limit curve along the prosthesis direction axis (0). This specific direction corresponds to the insertion axis of the initially prepared tooth mesh, which was defined during the dental prosthesis design on the dental CAD software. Then, the extruded surface is cut with a plane orthogonal to the insertion axis. Finally, the bottom open boundary is filled, and then the prepared tooth surfaces, extruded surfaces, and filling surfaces are joined to obtain a fully close geometrical model. The new bottom surface generated represents the basis of the preparation, where some mechanical boundary conditions will be applied.

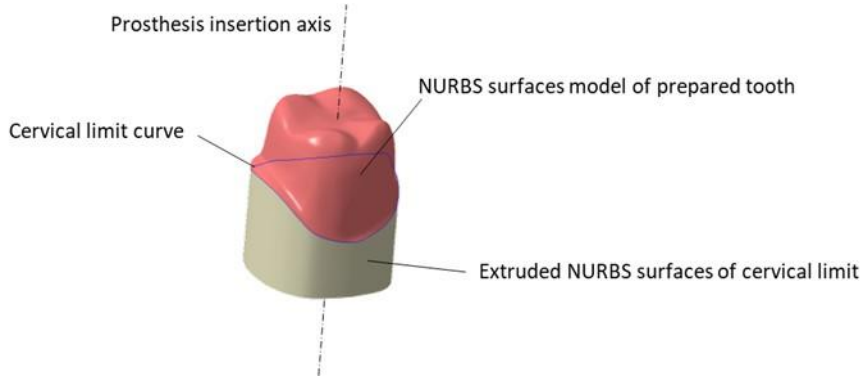

Figure 6: Final NURBS model of the prepared tooth.

2.2.4 Step 2.4: joint adhesive layer model generation

For the design of the thin joint adhesive layer, the cervical limit curve is first projected along the insertion axis direction onto the prosthesis shape (Figure 7.a). Then the projected curve is used to cut the geometry of the inner surface shape of the prosthesis (Figure 7.b). Finally, the open boundary between this new surface and the isolated prepared tooth surface is filled in. The three surfaces are joined to get a closed geometry describing the joint adhesive layer (Figure 7.c).

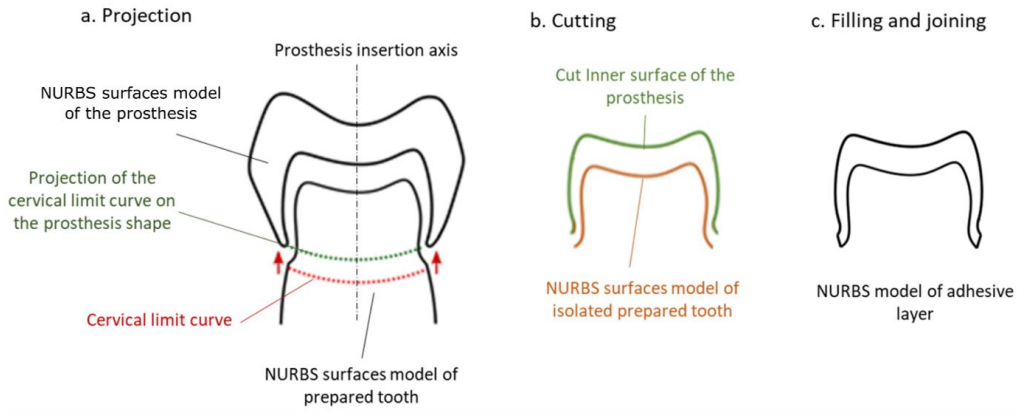

Figure 7: Adhesive layer CAD model generation.

2.3 Step 3: Mechanical Analysis of the Restoration Assembly

This section describes the five steps of the finite element modeling of the restored tooth assembly subjected to a mechanical loading (Figure 8). Most of the steps are performed independently. However, in the proposed method, the definition of the mechanically loaded zones is based on a modification of the CAD model, so the meshing step must be performed following it. No details concerning the method of calculation by finite element will be provided in this article. Interested readers will find more information in [3].

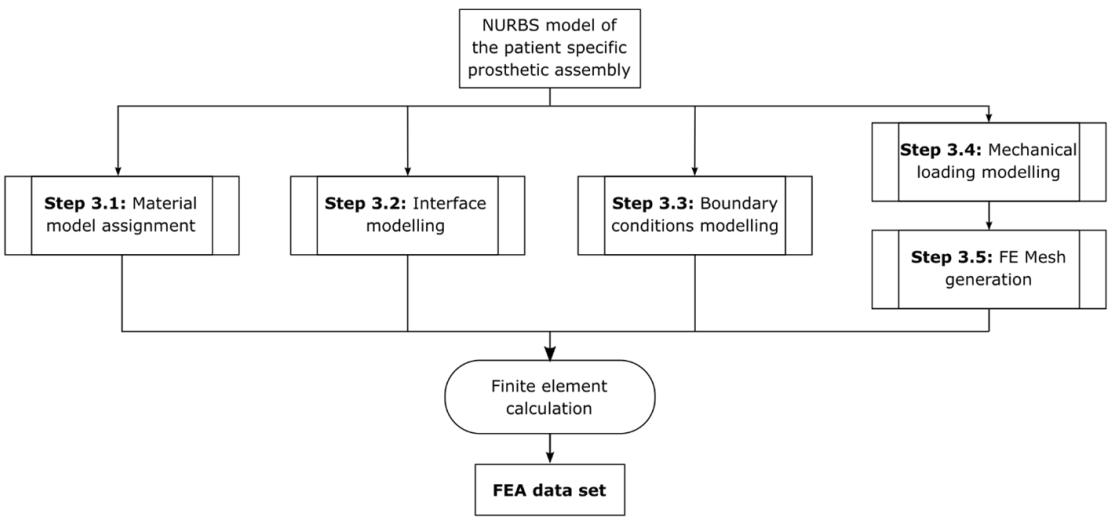

Figure 8: Mechanical modeling guidelines.

2.3.1 Step 3.1: material model assignment

In the studied assembly, three materials are considered: the ceramic (or glass-ceramic or hybrid ceramic) of the prosthesis, the adhesive layer made of resin material (resin with ceramic micro-fillers), and the dental preparation made of dentin (neglecting the possible presence of enamel).

For the mechanical analysis, the materials are assumed to have elastic linear isotropic behavior associated with a stress yield criterion (defining the elastic domain) or a strength criterion [29]. Indeed, i) no viscous or plasticity damage is expected during standard use, ii) the anisotropy of dental tissues is low and not well-known, and iii) describing a more complex behavior requires a major experimental investigation to collect the mechanical properties and increases the numerical calculation time. The mechanical properties of prosthesis biomaterial and of the adhesive material are usually provided by the manufacturers. The properties of dental tissues are available in the literature [54].

The dental preparation is simplified as a homogeneous tissue in elasticity and strength, while in reality, it is composed of both dentin and enamel remnants. Since this layer is separated from the prosthesis by an intermediate layer of adhesive sealant that is much softer (and thus will absorb the most deformation), we will assume that this usual simplification does not cause any disturbance in the location of the overstressed areas in the prosthesis.

2.3.2 Step 3.2: interface modeling

The mechanical behavior of bonded interfaces is complex and involves phenomena occurring at the microscale. It should be different at the prosthesis/adhesive layer interface and the adhesive layer/dentin interface. The models describing both are strongly nonlinear if the contacts between the surfaces are not perfect. This may occur as i) the defects of bonding due to the polymerisation process are not considered in this work [34,56] and ii) no damage of the thin adhesive layer is considered that may appear due to the repeated mechanical loading during mastication and the aging of the material.

However, for the application purpose, perfect interfaces between the adhesive layer and the other parts are considered, i.e., no relative displacement between the nodes at the interfaces (Figure. 9) in order to perform a calculation with a clinically reasonable amount of time.

2.3.3 Step 3.3: boundary conditions modeling

The tooth is anchored in the jaw via the periodontium, a thin set of tissues that transfers the force due to mastication, absorbs mechanical shocks and provides sensory input. Its mechanical behavior is viscoelastic, hyperelastic and anisotropic [40,62]. Within the usual framework of the dental CAD/CAM processes, the patient's tissue geometry is unknown. It may be obtained using a cone beam scanner, which is available in some practitioner offices.

In this preliminary design of the restorative dental assembly, this part in the FE simulations is considered to be unnecessary as the mechanical design is focused on the stress analysis in the prosthesis, which is sufficiently distanced from the periodontium. Moreover, its influence on the stress field distribution in the prosthesis and the adhesive layer under the applied load is limited. Thus, it is not taken into account in the following simulations where displacement boundary conditions are applied to the dental preparation (no displacement at the entire extrusion surface of the cervical line and to the base) (Figure 9).

2.3.4 Step 3.4: mechanical loading modeling

The current state of research on the subject does not make it possible to define a set of representative loads that is relevant for the mechanical study of dental prostheses. In this article, the global methodology is illustrated by considering only one representative loading, namely the contact between the two opposite teeth through chewed food. A method is proposed allowing, from the geometrical data of the patient, to define a surface where a uniform masticatory pressure is applied. This surface is extrapolated from the static relationship between the masticating surfaces

of the prosthesis and the antagonist teeth (Figure 10). In our work, we consider a single contact zone between the prosthesis and a tooth of the opposite dental arch.

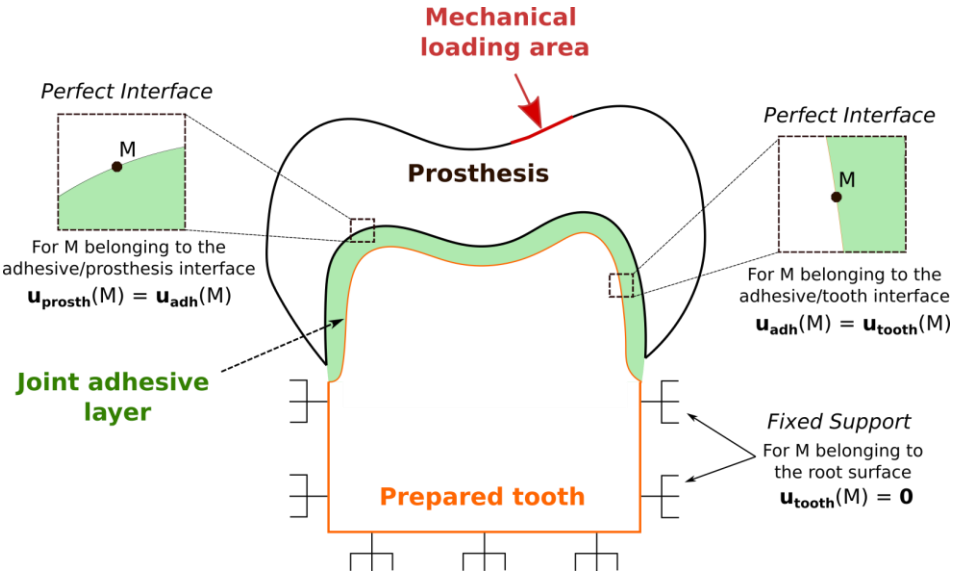

Figure 9: FEA boundary conditions (with $\mathbf{u_a}(M)$ the displacement vector of the domain a at the point M).

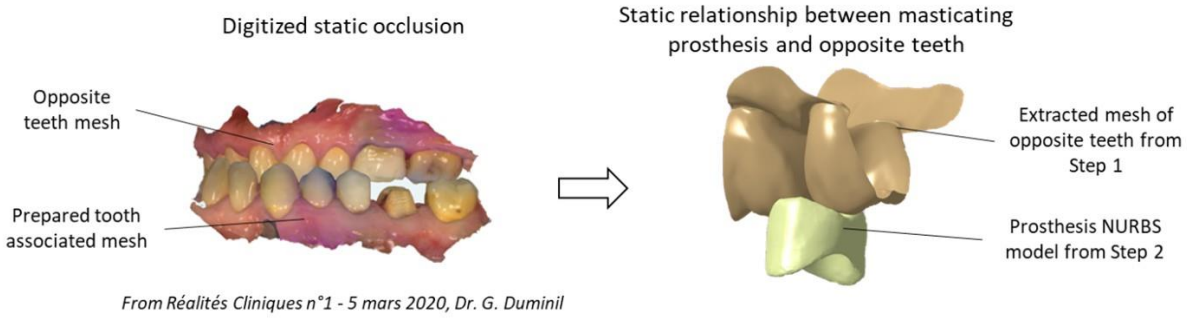

Figure 10: Static occlusion defined in the input data.

The loading surface is obtained using the extracted model of the prosthesis opposite tooth (Figure 11.a). A solid rigid kinematical translation of the opposite tooth along the prosthesis insertion axis is done to simulate tooth/prosthesis contact and to find the center of this intersection (Figure 11.b). Then, this point is used to define a centered radius disc that will be projected along the insertion axis onto the prosthesis surface (Figure 11.c). A 1mm radius disk and a 50MPa pressure loading were chosen in order to reproduce best a food chewing load [10].

In the case of a patient with two opposing teeth to be restored, the first step is to design the two restorations according to a current CAD/CAM protocol (based on geometric models of the teeth included in the software database). In a second step, the shape optimization would be performed, using the occlusion of the non-optimized prosthesis to define the mechanical loading surfaces.

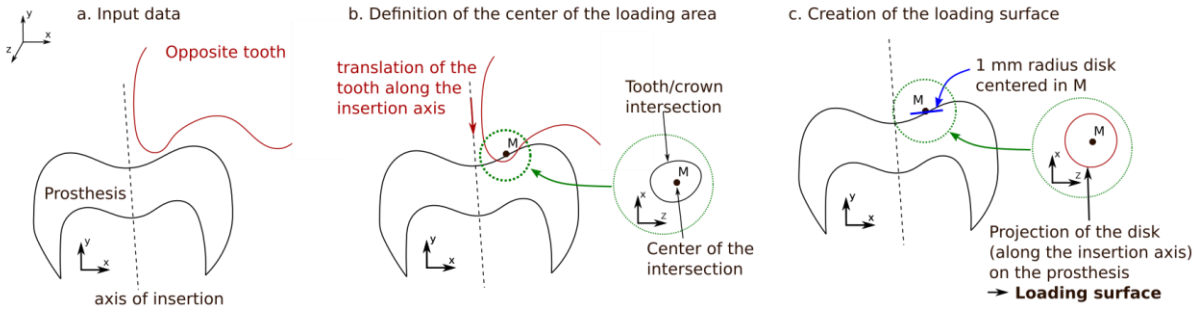

Figure 11: Design of the loading area.

2.3.5 Step 3.5: FE mesh generation

The restoration assembly geometry can be imported in common commercial FE codes (ANSIS, ABAQUS, ASTER, etc.) or owner-developed codes as the NURBS model can be embedded in an open file format such as STEP or IGES [44]. This geometry model is used to build the 3D FE mesh.

Due to the complex shape of the different assembly parts, a tetrahedral mesh generator is chosen [43]. A criterion based on the tetrahedral element radii ratio γ_K (i.e. the ratio between the inscribed and the circumcircles) was chosen to measure the quality of the mesh [16]:

$$\gamma_K = \frac{6\sqrt{6}V_K}{\left(\sum_{i=1}^{4} a(f_i)\right) \max\limits_{i=1,\dots,6} l(e_i)} \quad (2.\ 1)$$

with K the tetrahedral finite element, V_K the volume of K, $a(f_i)$ the aera of the i^{th} face of K and $l(e_i)$ the length of the i^{th} edge of K.

2.4 Mechanical and CAD Criteria

A method of structural shape optimization of the prosthesis is implemented in the proposed CAE tool (Figure 12).

The optimization problem is stated as finding the set of design variables, $\boldsymbol{X}$, that minimizes the objective function $F(\boldsymbol{X})$, $\boldsymbol{X}$ satisfying the constraints $g_j(\boldsymbol{X}) \leq 0$ with $j = 1, \dots, m$ and $X_i^L \leq X_i \leq X_i^U$(Vanderplaat, 1989). Design variables $\boldsymbol{X}$ may be of different nature (topology, material properties, etc.). Constraints $g_j(\boldsymbol{X}) \leq 0$ used in the proposed implementation are the limits imposed on stresses $\boldsymbol{\sigma}$ computed by FEA within the structure. They read $f_{y,j}(\boldsymbol{\sigma}) \leq 0$ associated to each material j of the assembly, $f_{y,j}(\boldsymbol{\sigma})$ being the yield or strength function. As dental materials are quasi-brittle, the yield criterion $f_{y,i}(\boldsymbol{\sigma}) \leq 0$ is based on the principal stresses $\sigma_I, \sigma_{II}, \sigma_{III}$ with $\sigma_I \geq \sigma_{II} \geq \sigma_{III}$.

Geometrical constraints $g_m(\boldsymbol{X}) \leq 0$ can also be introduced, such as non-penetration of the prosthesis outer surface into the adjacent or the tooth surfaces. Lower and upper values of the design variables X_i allow limiting the domain $\boldsymbol{X}$ to explore during the minimization process.

As a simple implementation, threshold values based on σ_I^{max} and σ_{II}^{max} could be defined. These threshold values, which are lower than the tensile yield strength of the material, make it possible to delay the fatigue failure of the structure [29].

2.5 Shape Optimization

The structural shape optimization procedure requires an appropriated parameterization of the geometry of the part to define the variables $\boldsymbol{X}$ [19,46]. Those are modified to minimize the stresses. In the case of a dental prosthesis obtained with standard CAD/CAM procedures, this parameterization is specific for each clinical case because the localization of the overstressed areas depends on the patient morphology and the position of the opposite teeth.

For the prosthesis made of brittle material such as ceramic, different areas might be considered for shape optimization:

(1) the inner surface of the prosthesis in contact with the joint adhesive layer where biaxial flexural stress occurs [35];

(2) the basis of the prosthesis, near the cervical limit, where tensile stress may occur [39];

(3) the upper surface of the prosthesis in contact with the opposite teeth and food and subjected to compressive loading [47].

This article introduces a method summarized in Figure 12 for the optimization case (1).

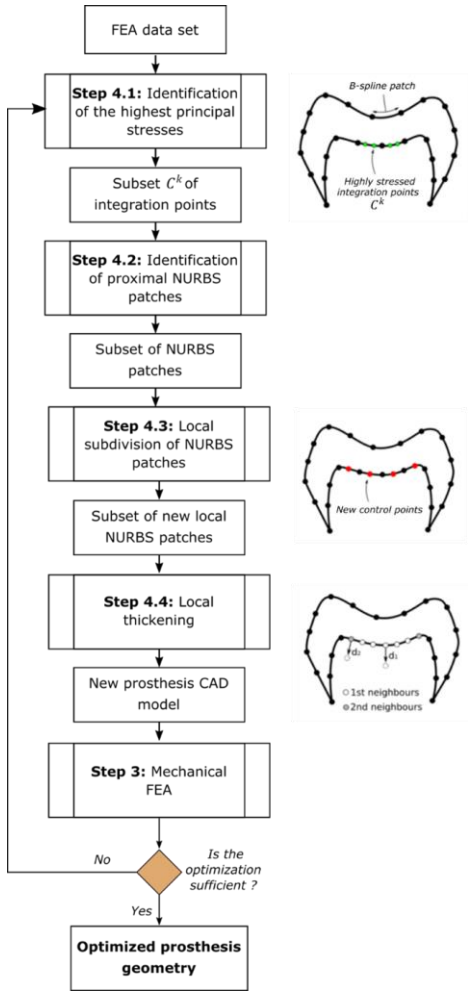

Figure 12: Prosthesis shape optimization.

When focusing the study on the joint adhesive layer where stress concentration exists, the geometry and mesh of this part need to be recomputed at each iteration of the optimization process. In order to facilitate the implementation, the geometrical modifications are taken on NURBS models rather than on finite elements meshes [27]. Re-meshing of the whole assembly is therefore made at each iteration *k* in order to perform the calculation.

At the given iteration k in the optimization process, the locations where σ_I^k and σ_{II}^k reach the highest values are targeted for surface changes (Step 4.1. in Figure 12). Considering the set I_p^k of the integration points p of the finite elements, a subset C^k is extracted according to the inequalities defined in the following equation, where γ_I and γ_{II} are arbitrarily parameters between 0 and 1:

$$C^k = \{\, p \in I_p^k \mid \sigma_I^k(p) \geq \gamma_I \, max(\sigma_I^k) \; and \; \sigma_{II}^k(p) \geq \gamma_{II} \, max(\sigma_{II}^k) \tag{2. 2}$$

Then, an initial subset S_i^k of NURBS patches in proximity with the subset C^k is identified on the CAD model (Step 4.2 in Figure 12). For each $p \in C^k$, the closest vertex v_p of the NURBS patches is located using Euclidian distance. Then, all the NURBS patches connected to v_p are added to S_i^k. S_i^k subset patches are subdivided in order to increase the points interpolating the NURBS geometry on the CAD model (Step 4.3. in Figure 12). This subdivision, defining a new subset S_j^k, is realized using the De Casteljeau algorithm [44].

To modify the prosthesis geometry, a local thickening of the inner shape is performed by modifying the positions of the interpolating points q_j of the subset S_j^k. The nearest vertices of the NURBS patches from the set C^k are identified in the first neighbors set $Nset_1^k$. The vertices sharing a NURBS patch with the vertices in $Nset_1$ are identified in the second neighbors set $Nset_2^k$.

The interpolating points q_j are moved as follow (Figure 13):

- if $q_j \in Nset_2^k$, where $Nset_2^k$ is the second neighbors set, p_j is offset on the local normal direction of a distance d_2,
- if $q_j \in Nset_1^k$, where $Nset_1^k$ is the first neighbors set, p_j is offset on the local normal direction of a distance d_1 with $d_1 > d_2$.

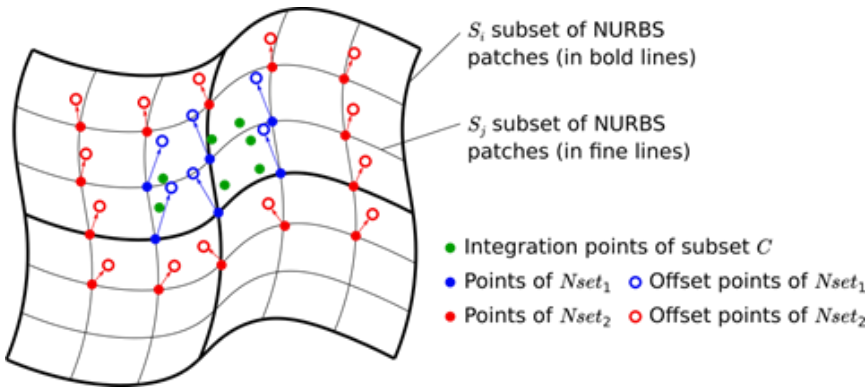

Figure 13: NURBS surface modification.

Thus, d_1 and d_2 are thickening parameters for the optimization procedure. These parameters are constrained, as the gap between the prosthesis and the prepared tooth should not be less than an arbitrary value to let a reliable space for adhesive biomaterial. A new CAD model and FE mesh of the prosthetic restoration assembly are therefore built and FEA is run to compute the σ_I^{k+1} and σ_{II}^{k+1}. If the stress levels σ_I^{k+1} and σ_{II}^{k+1} are considered too high, a local iterative loop is processed in order to find optimum values for d_1 and d_2. The end of the process is defined by an arbitrary criterion, such as a norm of determining if the optimization is sufficient for the user.

3 IMPROVEMENT OF A CLINICAL CASE

The CAE approach was experienced on a real clinical situation. First, a mandibular second premolar prosthetic restoration was prepared and designed with a commercial dental CAD/CAM system by a professional dentist. Then, the designed crown restoration was optimized with our CAE tool.

The different steps performed in this part could be automated in a calculation code specific to the mechanical optimization of dental prostheses. However, the proof of concept developed below has been carried out using proprietary tools. Most of the CAD operations were performed using CATIA V5 software (Dassault System, Velizy Vilacoublay), with the exception of the reverse-engineering algorithm, and the FE calculations were performed using ABAQUS 6.11 software (Dassault System, Velizy Vilacoublay).

3.1 Patient-Specific Extracted Data – Step 1

The prepared premolar and its environment were digitized using a Carestream CS 3600 intraoral scanner (Carestream Dental, Atlanta, GA). The Figure 14.a illustrates the two meshes used as input data in our CAE tool. In our example, the two meshes were stored in STL file format.

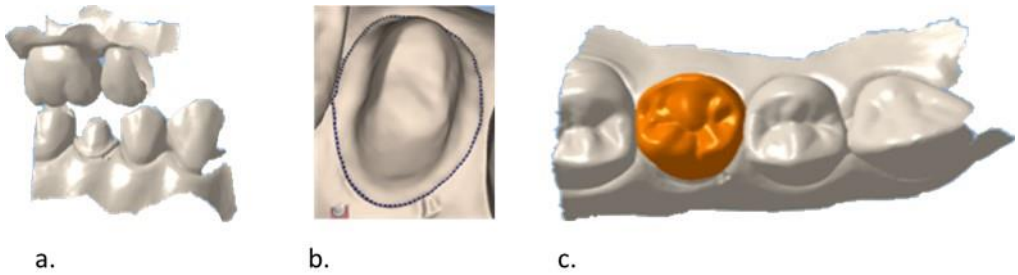

Figure 14: Extracted data embedded in dental CAD/CAM process - a. adjacent and opposite teeth meshes - b. dental preparation and cervical limit curve - c. crown CAD model.

The CAD/CAM software Romexis PlanMeca 4.1.2 (Planmeca, Helsinki, Finland) was used to design the model of a prosthetic crown. First, the curve defining the cervical limit of the prepared tooth was semi-automated designed by the dentist. The Figure 14.b illustrates the B-spline curve modeling the cervical limit. In this example, the B-spline curve was stored in IGES file format.

Then, a premolar anatomy was selected in the software database by the dentist to define the outer shape of the crown. This selection was not computer-assisted; the dentist choice was based on the analysis of the symmetric premolar supposed to be quite similar to the premolar to be restored. To design the inner shape of the crown, the gap between the crown and the dental preparation was set to 200 µm to simulate the space needed for the adhesive material. Based on these parameters and models, a first crown CAD model was automatically designed. Finally, based on the dentist experience, the outer shape of the crown was modified with CAD geometrical operators to adjust the occlusal contact with opposite teeth and the proximal contact with the adjacent teeth. Figure. 14.c illustrates the crown CAD model positioning on the prepared tooth. For the specific commercial software used in our work, the CAD model of the crown was a mesh embedded in a STL file format.

3.2 CAD Model Generation - Step 2

First, to isolate the prepared tooth point cloud, the extracted B-spline curve, representing the cervical limit, was used as cutting element of the associated prepared tooth mesh (Step 2.1 in section 2.2.1). Then, the isolated prepared tooth mesh and the prosthesis shape mesh extracted from the dental CAD software are associated to NURBS surfaces using the reverse-engineering algorithm

(Step 2.2 in section 2.2.2). To generate the final NURBS model of the prepared tooth, the cervical limit curve was used to generate an extrusion surface along the prosthesis insertion axis direction (Step 2.3 in section 2.2.3). The length of extrusion was set to 10 mm to avoid boundary effects during the mechanical analysis. Finally, the joint adhesive layer shape was generated according to geometrical operations detailed in section 2.2.4 (Step 2.4). The resulting NURBS models of the restoration assembly are illustrated in Figure 15.

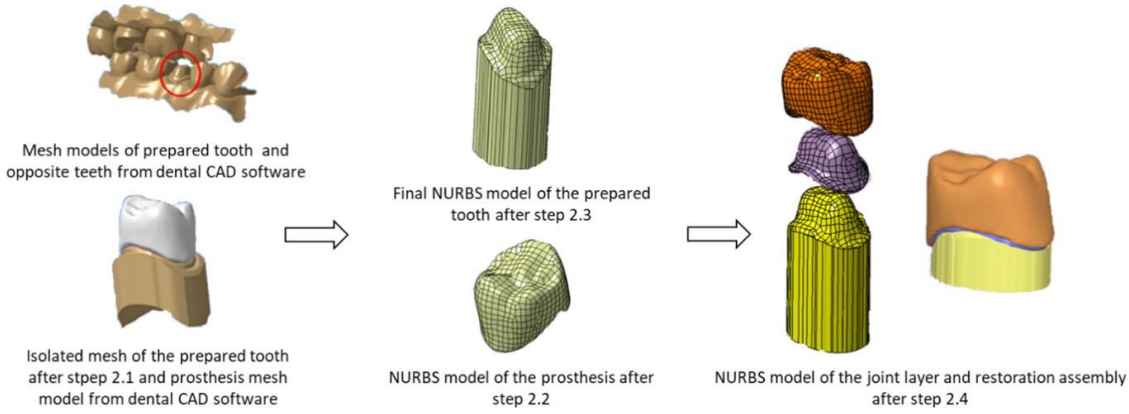

Figure 15: Restoration assembly NURBS models generated.

3.3 Mechanical Analysis – Step 3

3.3.1 Material model assignment – Step 3.1

To set the elastic linear isotropic properties of each material domain, representative and commonly used in clinic biomaterials were chosen to model the behavior of a leucite reinforced feldspathic glass-ceramic for the prosthesis, a composite polymeric resin for the joint adhesive layer and the human dentin for the prepared tooth [18,23,54]. The material properties are detailed in Table. 1.

Material	*Young's modulus (GPa)*	*Poisson's ratio*	*Yield strength (MPa)*
Prosthesis: glass ceramic	80	0.3	300
Adhesive layer: composite resin	5	0.35	130
Prepared tooth: human dentin	18,3	0.25	100

Table 1: Elastic linear isotropic properties set in FE model.

3.3.2 Displacement constraints implementation – Steps 3.2 – 3.3

Tied contacts were modeled between the prosthesis and adhesive layer and between the prepared tooth and adhesive layer using the "Tie constraint" function of ABAQUS software in which the constraints are enforced with a direct Lagrange multiplier method (section 2.3.2). Zero displacements were prescribed on the nodes belonging to the base and the root-like surfaces of the tooth preparation (section 2.3.3).

3.3.3 Generated opposite teeth contact model – Step 3.4

The following CAD operations were taken with the CATIA V5 software. The method is detailed in section 2.3.4. In the studied clinical configuration, a 3mm translation along the crown insertion axis

has simulated the dynamic occlusion (Figure 16.a). The resulting intersection surface between the crown and the opposite teeth is illustrated in Figure. 16.b. A 1mm radius disk was defined in a plane perpendicular to the prosthesis insertion axis and centered on the centre of inertia of the surface intersection. This disk projected onto the crown surface defined the loading area (Figure 16.c). A uniform 50 MPa normal pressure was applied on it [10].

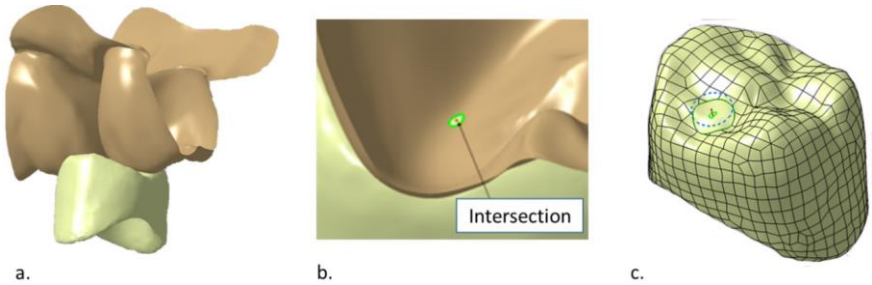

Figure 16: Patient-specific designed loaded area.

3.3.4 FE mesh generation – Step 3.5

The STEP file of the restoration assembly was imported into the FEA software ABAQUS 6.11. The meshing algorithm performed was the "free method" for each part of the restoration assembly. Second-order tetrahedral elements (C3D10) were used to limit the number of elements considering the complex geometry of the restoration assembly parts. The resulting mesh characteristics are presented in Table 2.

Part	*Number of elements*	*Average length (mm)*	γ_K
Crown	336047	0.17	0.68
Adhesive layer	170849	0.09	0.7
Prepared tooth	80783	0.37	0.68

Table 2: FE Mesh characteristics

3.3.5 Initial mechanical simulation results

The presented initial mechanical analysis ($k = 1$) is focused on the first maximum principal stress in the crown as primary data for mechanical optimization, as the tensile strength of ceramics is much lower than the compression strength.

Three areas highly solicited by tensile stress are shown in Figure 17: (i) ROI 1 located at the border of the loading area; (ii) ROI 2 located on the cervical limit of the restoration; iii) ROI 3 located at the junction with the joint adhesive layer underneath the loading area. These three overstressed areas illustrate the main clinical failure patterns of ceramic dental restorations already identified in Section 2.5.

In ROI 1, the presence of high tensile stresses is directly related to the imposed mechanical loading. In this area, σ_I^1 reaches 20 MPa. The ROI 2 located on the bucco-lingual wall of the prosthesis shows tensile stresses with σ_I^1 reaching 12 MPa. The corresponding principal direction is approximately tangent to the cervical line, thus the application of loading generates circumferential tensile stresses at the basis of the prosthesis. The tensile stresses are the highest in ROI 3 with $\sigma_I^1 \approx 26$ MPa and $\sigma_{II}^1 \approx 21$ MPa. This area is subject to biaxial tensile stress created by the bending of the upper part of the prosthesis.

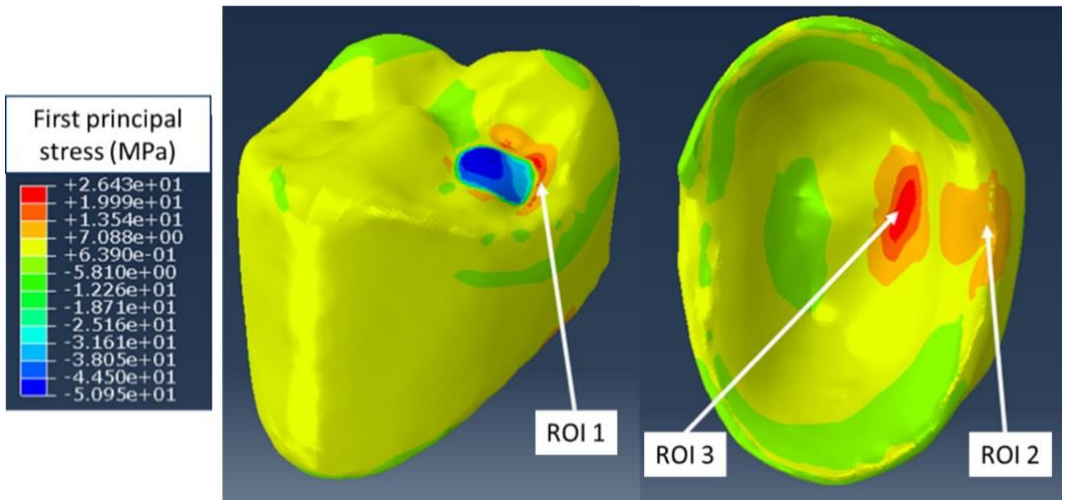

Figure 17: Maximum principal stress within the crown (ROI: Region of Interest).

According to this analysis, the specific portion, close to ROI 3 of the inner shape of the crown was targeted for the geometrical optimization according to the procedure detailed in section 2.5.

3.4 Mechanically Improved Patient Specific Prosthesis – Step 4

The aim of this step is to reduce the mechanical stresses in the prosthetic part while defining dimensional constraints on the CAD model of the adhesive joint layer (herein 50 µm).

The optimization process for the patient specific crown studied is illustrated in Figure 18. The subset C^0 of the integration points, where σ_I^1 and σ_{II}^1 reached values higher than 70% of the maximal values was defined ($\gamma_I = 0.7$ and $\gamma_{II} = 0.7$) (Figure 18.a). Then, the NURBS patches in proximity with the integration points were localized and subdivided (Figure 18.b). Finally, a local shape thickening was performed after the two neighbours classifications by offsetting the subdivided patches boundaries, with the parameters $d_1 = 150\ \mu m$ in the central subdivided patches (1st neighbor, NSet1) and $d_2 = 75\ \mu m$ in the median subdivided patches (2nd neighbor, NSet2). The resulting local thickening is illustrated on a cutting plane in Figure 18.c.

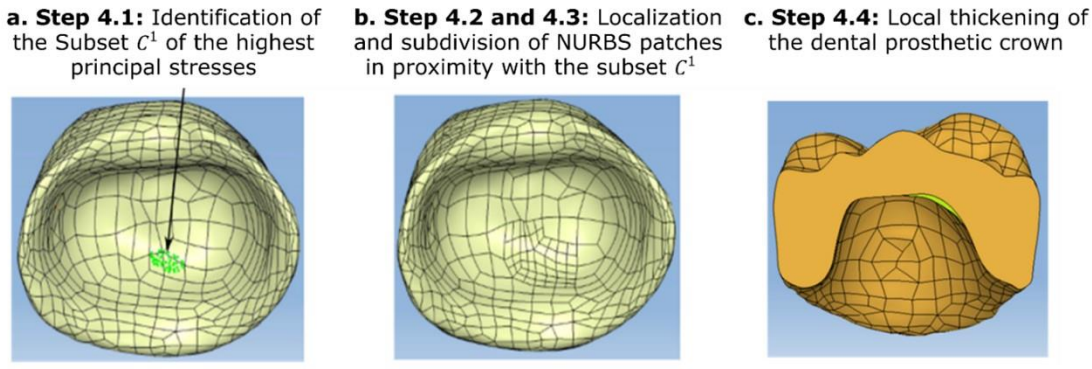

Figure 18: Optimization process steps on the patient-specific crown.

After local shape modification, a new FEA was conducted on the new restoration assembly (iteration $k = 2$). As illustrated in Figure 19, the inner prosthesis shape modification helps to decrease the maximal first principal stresses in ROI 3. Whereas in ROI 1 and ROI 2, the stress reductions are negligible compared to the first prosthesis design. These preliminary results emphasize the relevance to locally modify the prosthesis to reduce potential high stresses that may lead to potential prosthetic restoration failure. In this case, in ROI 3 σ_I^2 reaches approx. 20 MPa and σ_{II}^2 reaches approx. 17 MPa, which corresponds to a decrease of 23% and 19 % respectively for σ_I and σ_{II}.

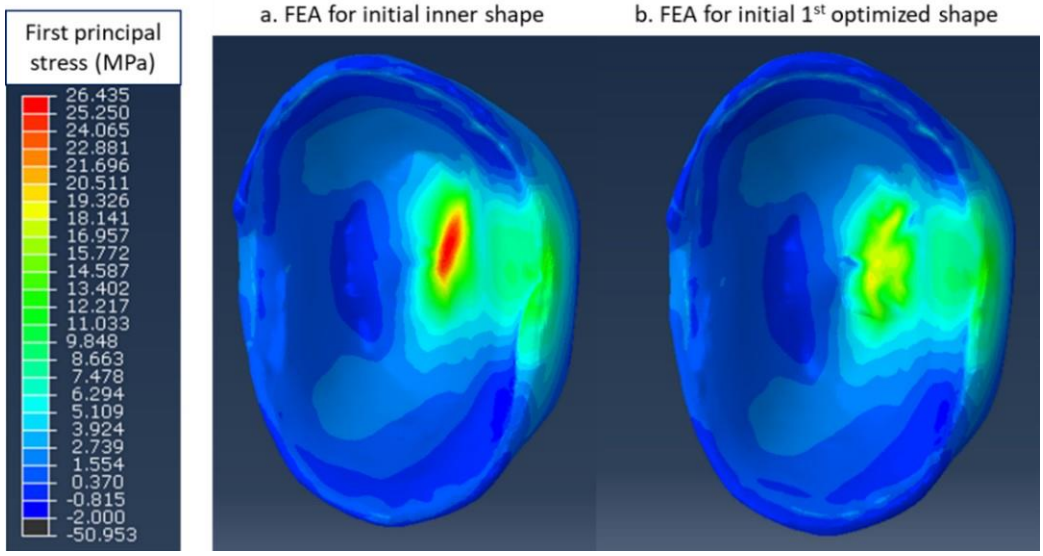

Figure 19: Comparison of 1st principal stress on the inner shape ROI 3 before and after improvement.

4 PERSPECTIVES

The exposed digital chain is a first step in developing a tool encompassing both the improved geometric optimization of restorative dental assemblies and the estimation of the lifetime of such assemblies. It offers a strong growth potential to develop innovative solutions. Several developments are possible either to improve the accuracy of the FE simulation or to improve the tool:

- define a relevant criterion to validate or not the optimized shape of the prosthesis: how to answer the question "is the optimization sufficient?" in Figure. 12;
- carrying out FE simulations with different load histories representative of the mastication to refine the location of the critical zones of stress concentration;
- refining constitutive equations for the materials in particular, taking into account fatigue behavior which is needed to improve the longevity of prostheses;
- taking into account more efficient tools developed more recently in the field of topological optimization [21] and the numerical mechanical analyses with strongly reduced computational times e.g. Proper generalized decomposition [5].

Mechanical considerations might also guide the choice of the prosthesis biomaterial and the adhesive biomaterial as it exists a wide variety of restorative materials with different mechanical properties, making difficult their choices during prosthesis design process.

5 CONCLUSIONS

In restorative dentistry, engineering tools such as CAD/CAM technologies are used for patient-specific prosthesis design and manufacturing. The dentist skills focus on therapeutic and health considerations, whereas the dental technician skills focus on know-how on shaping biomaterials. Each prosthesis is unique and can be considered as a prototype to respond to a specific clinical situation.

The prosthesis design process is commonly limited to geometrical constraints, and surprisingly, no mechanical considerations are taken into account. In this paper, a CAE methodology is proposed and an automated CAE tool developed in the field of all-ceramic restorative dentistry. For the first time, a mechanical analysis is embedded in the dental prosthesis CAD workflow. It does not necessitate any supplementary handling from the dentist nor any advanced mechanical engineering skills. So, this work perfectly fits with the "smart healthcare" concept by providing patient-specific optimized solutions for dentistry.

The present work highlights that data embedded in current dental CAD/CAM systems can be used to provide a finite elements analysis usable for design optimization with a high level of automation. In response to in-vitro and in-vivo studies underlying the weakness of dental prostheses, a methodology is outlined to enhance the design of the inner shape of dental prosthetic restorations by locally reducing tensile stresses. The developed CAE tool was successfully applied on a real tooth restoration. It demonstrates that significant improvements may be expected in dental design. It can be easily extended to other critical areas such as cervical limit, other mechanical criteria such as shear criteria on the adhesive joint/prosthesis interface, or other types of all-ceramic fixed partial denture prosthesis such as inlay, onlay, or overlay.

ACKNOWLEDGMENT

This work has benefited from the financial support of the LabeX LaSIPS (ANR-10-LABX-0040-LaSIPS) managed by the French National Research Agency under the "Investissements d'avenir" program (n°ANR-11-IDEX-0003-02).

Kyo Shindo, https://orcid.org/0000-0003-2120-9711
Laurent Tapie, https://orcid.org/0000-0002-6857-441X
Nicolas Schmitt, https://orcid.org/0000-0001-5723-8958
Elsa Vennat, https://orcid.org/0000-0002-3957-7742

REFERENCES

[1] Blatz, M.B.; Conejo, J.: The Current State of Chairside Digital Dentistry and Materials, Dental Clinics of North America, 63(2), 2019, 175–97. https://doi.org/10.1016/j.cden.2018.11.002
[2] Bowley, J.F.; Ichim, I.P.; Kieser, J.A.; Swain, M.V.: FEA evaluation of the resistance form of a premolar crown, Journal of Prosthodontics, 22(4), 2013, 304–12. https://doi.org/10.1111/j.1532-849X.2012.00949.x
[3] Chandrupatla, T.R.; Belegundu, A.D.: Introduction to finite elements in engineering, Englewood Cliffs, N.J: Prentice-Hall
[4] Chang, M.; Oh, J.W.; Park, S.C.: Next viewing directions for the scanning of dental impressions, Computer-Aided Design, 66, 2015, 24–32. https://doi.org/10.1016/j.cad.2015.04.007
[5] Chinesta, F.; Leygue, A.; Bordeu, F.; Aguado, J.V.; Cueto, E.; Gonzalez, D.; Alfaro, I.; Ammar, A.; Huerta, A.: PGD-Based Computational Vademecum for Efficient Design, Optimization and Control Archives of Computational Methods in Engineering, 20(1), 2013, 31–59. https://doi.org/10.1007/s11831-013-9080-x
[6] Christensen, C.: Food texture perception, Advances in Food Research, 29, Elsevier, 159–99, 1984. https://doi.org/10.1016/S0065-2628(08)60057-9

[7] Clelland, N.L.; Ramirez, A.; Katsube, N.; Seghi, R.R.: Influence of bond quality on failure load of leucite-and lithia disilicate–based ceramics, The Journal of Prosthetic Dentistry, 97(1), 2007, 18–24. https://doi.org/10.1016/j.prosdent.2006.11.009
[8] Dan, J.; Lancheng, W.: An algorithm of NURBS surface fitting for reverse engineering, The International Journal of Advanced Manufacturing Technology, 31(1-2), 2006, 92–7. https://doi.org/10.1007/s00170-005-0161-3
[9] Davidowitz, G.; Kotick, P.G.: The use of CAD/CAM in dentistry, Dental Clinics, 55(3), 2011, 559–70. https://doi.org/10.1016/j.cden.2011.02.011
[10] Dejak, B.; Młotkowski, A.; Romanowicz, M.: Finite element analysis of stresses in molars during clenching and mastication, The Journal of Prosthetic Dentistry, 90(6), 2003, 591–7. https://doi.org/10.1016/j.prosdent.2003.08.009
[11] Dong, X.; Darvell, B.: Stress distribution and failure mode of dental ceramic structures under Hertzian indentation, Dental Materials, 19(6), 2003, 542–51. https://doi.org/10.1016/S0109-5641(02)00103-3
[12] Dupagne, L.; Tapie, L.; Lebon, N.; Mawussi, B.: Comparison of the acquisition accuracy and digitizing noise of 9 intraoral and extraoral scanners: An objective method, The Journal of Prosthetic Dentistry, 2021. https://doi.org/10.1016/j.prosdent.2021.02.005
[13] Falck, B.; Falck, D.; Collette, B.: Freecad [How-To. Packt Publishing Ltd
[14] Farin, G.: From conics to NURBS: A tutorial and survey, IEEE Computer Graphics and Applications, 12(5), 1992, 78–86. https://doi.org/10.1109/38.156017
[15] Gaspar, M.; Weichert, F.: Integrated construction and simulation of tool paths for milling dental crowns and bridges, Computer-Aided Design, 45(10), 2013, 1170–81. https://doi.org/10.1016/j.cad.2013.04.007
[16] Geuzaine, C.; Remacle, J.-F.: Gmsh: a three-dimensional finite element mesh generator with built-in pre- and post-processing facilities, International Journal for Numerical Methods in Engineering, 79(11), 2009, 1309-1331. https://doi.org/10.1002/nme.2579
[17] Goodacre, C.J.; Bernal, G.; Rungcharassaeng, K.; Kan, J.Y.K.: Clinical complications in fixed prosthodontics, The Journal of Prosthetic Dentistry, 90(1), 2003, 31–41. https://doi.org/10.1016/S0022-3913(03)00214-2
[18] Habelitz, S.; Marshall, S.; Marshall Jr, G.; Balooch, M.: Mechanical properties of human dental enamel on the nanometre scale, Archives of Oral Biology, 46(2), 2001, 173–83. https://doi.org/10.1016/S0003-9969(00)00089-3
[19] Hardee, E.; Chang, K.-H.; Tu, J.; Choi, K.K.; Grindeanu, I.; Yu, X.: A CAD-based design parameterization for shape optimization of elastic solids, Advances in Engineering Software, 30(3), 1999, 185–99. https://doi.org/10.1016/S0965-9978(98)00065-9
[20] Heintze, S.; Cavalleri, A.; Zellweger, G.; Büchler, A.; Zappini, G.: Fracture frequency of all-ceramic crowns during dynamic loading in a chewing simulator using different loading and luting protocols, Dental Materials, 24(10), 2008, 1352–61. https://doi.org/10.1016/j.dental.2008.02.019
[21] Henrot, A.; Pierre, M.: Shape variation and optimization: A geometrical analysis, Zürich: European Mathematical Society
[22] Hidaka, O.; Iwasaki, M.; Saito, M.; Morimoto, T.: Influence of clenching intensity on bite force balance, occlusal contact area, and average bite pressure, Journal of Dental Research, 78(7), 1999, 1336–44. https://doi.org/10.1177/00220345990780070801
[23] Ilie, N.; Hickel, R.: Investigations on mechanical behaviour of dental composites, Clinical Oral Investigations, 13(4), 2009, 427. https://doi.org/10.1007/s00784-009-0258-4
[24] Kelly, J.R.; Nishimura, I.; Campbell, S.D.: Ceramics in dentistry: Historical roots and current perspectives, The Journal of Prosthetic Dentistry, 75(1), 1996, 18–32. https://doi.org/10.1016/S0022-3913(96)90413-8
[25] Kim, J.H.; Miranda, P.; Kim, D.K.; Lawn, B.R.: Effect of an adhesive interlayer on the fracture of a brittle coating on a supporting substrate, Journal of Materials Research, 18(1), 2003, 222–7. https://doi.org/10.1557/JMR.2003.0031

[26] Koolstra, J.H.; Eijden, T.M.: The jaw open-close movements predicted by biomechanical modelling, Journal of Biomechanics, 30(9), 1997, 943–50. https://doi.org/10.1016/S0021-9290(97)00058-4
[27] Laporte, E.; Le Tallec, P.: Numerical methods in sensitivity analysis and shape optimization. Springer Science & Business Media.
[28] Lebon, N.; Tapie, L.; Duret, F.; Attal, J.-P.: Understanding dental CAD/CAM for restorations - dental milling machines from a mechanical engineering viewpoint. Part A: chairside milling machines, International Journal of Computerized Dentistry, 19(1), 2016, 45–62.
[29] Lemaître, J.; Desmorat, R.: Engineering Damage Mechanics: Ductile, Creep, Fatigue and Brittle Failures. Softcover reprint of hardcover 1st, Springer-Verlag.
[30] Liu, B.; Lu, C.; Wu, Y.; Zhang, X.; Arola, D.; Zhang, D.: The Effects of Adhesive Type and Thickness on Stress Distribution in Molars Restored with All-Ceramic Crowns, Journal of Prosthodontics: Implant, Esthetic and Reconstructive Dentistry, 20(1), 2011, 35–44. https://doi.org/10.1111/j.1532-849X.2010.00650.x
[31] Ma, W.; Kruth, J.-P.: NURBS curve and surface fitting for reverse engineering, The International Journal of Advanced Manufacturing Technology, 14(12), 1998, 918–27. https://doi.org/10.1007/BF01179082
[32] Maghami, E.; Homaei, E.; Farhangdoost, K.; Pow, E.H.N.; Matinlinna, J.P.; Tsoi, J.K.-H.: Effect of preparation design for all-ceramic restoration on maxillary premolar: A 3D finite element study, Journal of Prosthodontic Research, 62(4), 2018, 436–42. https://doi.org/10.1016/j.jpor.2018.04.002
[33] Mahant, R.; Agrawal, S.; Kapoor, S.; Agrawal, I.: Milestones of dental history, CHRISMED Journal of Health and Research, 4(4), 2017, 229. https://doi.org/10.4103/cjhr.cjhr_37_17
[34] May, L.G.; Kelly, J.R.: Influence of resin cement polymerization shrinkage on stresses in porcelain crowns, Dental Materials: Official Publication of the Academy of Dental Materials, 29(10), 2013, 1073–9. https://doi.org/10.1016/j.dental.2013.07.018
[35] May, L.G.; Kelly, J.R.; Bottino, M.A.; Hill, T.: Effects of cement thickness and bonding on the failure loads of CAD/CAM ceramic crowns: Multi-physics FEA modeling and monotonic testing, Dental Materials, 28(8), 2012, 99–109. https://doi.org/10.1016/j.dental.2012.04.033
[36] Miura, S.; Kasahara, S.; Yamauchi, S.; Egusa, H.: Effect of finish line design on stress distribution in bilayer and monolithic zirconia crowns: a three-dimensional finite element analysis study, European Journal of Oral Sciences, 126(2), 2018, 159–65. https://doi.org/10.1111/eos.12402
[37] Mondy, W.L.; Cameron, D.; Timmermans, J.P.; De Clerck, N.; Sasov, A.; Casteleyn, C.; Piegl, L.A.: Computer-aided design of microvasculature systems for use in vascular scaffold production, Biofabrication, 1(3), 2009, 035002. https://doi.org/10.1088/1758-5082/1/3/035002
[38] Moörmann, W.H.: The evolution of the CEREC system, The Journal of the American Dental Association, 137, 2006, 7–13. https://doi.org/10.14219/jada.archive.2006.0398
[39] Nasrin, S.; Katsube, N.; Seghi, R.; Rokhlin, S.: Survival predictions of ceramic crowns using statistical fracture mechanics, Journal of Dental Research, 96(5), 2017, 509–15. https://doi.org/10.1177/0022034516688444
[40] Natali, A.N.; Pavan, P.G.; Scarpa, C.: Numerical analysis of tooth mobility: formulation of a nonlinear constitutive law for the periodontal ligament, Dental materials: official publication of the Academy of Dental Materials, 20(7), 2004, 623–9. https://doi.org/10.1016/j.dental.2003.08.003
[41] Øilo, M.; Hardang, A.D.; Ulsund, A.H.; Gjerdet, N.R.: Fractographic features of glass-ceramic and zirconia-based dental restorations fractured during clinical function, European Journal of Oral Sciences, 122(3), 2014, 238–44. https://doi.org/10.1111/eos.12127
[42] Oliphant, T.: Guide to NumPy, CreateSpace Independent Publishing Platform, Austin, TX, 2015
[43] Parthasarathy, V.N.; Graichen, C.M.; Hathaway, A.F.: A comparison of tetrahedron quality measures, Finite Elements in Analysis and Design, 15(3), 1994, 255–61. https://doi.org/10.1016/0168-874X(94)90033-7

[44] Piegl, L.; Tiller, W.: The NURBS Book, Springer-Verlag, 1995. https://doi.org/10.1007/978-3-642-97385-7
[45] Sailer, I.; Makarov, N.A.; Thoma, D.S.; Zwahlen, M.; Pjetursson, B.E.: All-ceramic or metal-ceramic tooth-supported fixed dental prostheses (FDPs)? A systematic review of the survival and complication rates. Part I: Single crowns (SCs, Dental Materials, 31(6), 2015, 603–23. https://doi.org/10.1016/j.dental.2015.02.011
[46] Samareh, J.A.: Survey of shape parameterization techniques for high-fidelity multidisciplinary shape optimization, AIAA journal, 39(5), 2001, 877–84. https://doi.org/10.2514/2.1391
[47] Scherrer, S.S.; Quinn, J.B.; Quinn, G.D.; Kelly, J.R.: Failure analysis of ceramic clinical cases using qualitative fractography., International Journal of Prosthodontics, 19(2), 2006
[48] Song, Y.-L.; Li, J.; Yin, L.; Huang, T.; Gao, P.: The feature-based posterior crown design in a dental CAD/CAM system, The International Journal of Advanced Manufacturing Technology, 31(11-12), 2007, 1058–65. https://doi.org/10.1007/s00170-005-0289-1
[49] Sornsuwan, T.; Swain, M.V.: The effect of margin thickness, degree of convergence and bonding interlayer on the marginal failure of glass-simulated all-ceramic crowns, Acta Biomaterialia, 8(12), 2012, 4426–37. https://doi.org/10.1016/j.actbio.2012.08.006
[50] Tapie, L.; Chiche, N.; Boitelle, P.; Morenton, P.; Attal, J.-P.; Schmitt, N.; Vennat, E.: Adaptation Measurement of CAD/CAM Dental Crowns with X-Ray Micro-CT: Metrological Chain Standardization and 3D Gap Size Distribution, Advances in Materials Science and Engineering, 2016, 2016, 1–13. https://doi.org/10.1155/2016/7963928
[51] Tapie, L.; Lebon, N.; Mawussi, B.; Fron Chabouis, H.; Duret, F.; Attal, J.-P.: Understanding dental CAD/CAM for restorations--the digital workflow from a mechanical engineering viewpoint, International Journal of Computerized Dentistry, 18(1), 2015, 21–44.
[52] Thompson, J.; Anusavice, K.; Naman, A.; Morris, H.: Fracture surface characterization of clinically failed all-ceramic crowns, Journal of Dental Research, 73(12), 1994, 1824–32. https://doi.org/10.1177/00220345940730120601
[53] Tsai, Y.-L.; Petsche, P.E.; Anusavice, K.J.; Yang, M.C.: Influence of glass-ceramic thickness on Hertzian and bulk fracture mechanisms., International Journal of Prosthodontics, 11(1), 1998
[54] Wang, W.; Roubier, N.; Puel, G.; Allain, J.-M.; Infante, I.C.; Attal, J.-P.; Vennat, E.: A new method combining finite element analysis and digital image correlation to assess macroscopic mechanical properties of dentin, Materials, 8(2), 2015, 535–50. https://doi.org/10.3390/ma8020535
[55] Wassell, R.W.; Steele, J.G.; Welsh, G.: Considerations when planning occlusal rehabilitation: A review of the literature, International Dental Journal, 48(6), 1998, 571–81. https://doi.org/10.1111/j.1875-595X.1998.tb00494.x
[56] Yasothan, Y.; Shindo, K.; Schmitt, N.; Vennat, E.: Morphological characterization of defects in all-ceramic crown adhesive layer, Computer Methods in Biomechanics and Biomedical Engineering, 23, 2020, 303–5. https://doi.org/10.1080/10255842.2020.1816302
[57] Yoo, D.-J.: Three-dimensional surface reconstruction of human bone using a B-spline based interpolation approach, Computer-Aided Design, 43(8), 2011, 934–47. https://doi.org/10.1016/j.cad.2011.03.002
[58] Yuwen, S.; Dongming, G.; Zhenyuan, J.; Weijun, L.: B-spline surface reconstruction and direct slicing from point clouds, The International Journal of Advanced Manufacturing Technology, 27(9-10), 2006, 918–24. https://doi.org/10.1007/s00170-004-2281-6
[59] Zhang, Z.; Sornsuwan, T.; Rungsiyakull, C.; Li, W.; Li, Q.; Swain, M.V.: Effects of design parameters on fracture resistance of glass simulated dental crowns, Dental Materials, 32(3), 2016, 373–84. https://doi.org/10.1016/j.dental.2015.11.018
[60] Zheng, S.-X.; Li, J.; Sun, Q.-F.: A novel 3D morphing approach for tooth occlusal surface reconstruction, Computer-Aided Design, 43(3), 2011, 293–302. https://doi.org/10.1016/j.cad.2010.11.003
[61] Zheng, S.-X.; Li, J.; Sun, Q.-F.: A novel 3D morphing approach for tooth occlusal surface reconstruction, Computer-Aided Design, 43(3), 2011, 293–302. https://doi.org/10.1016/j.cad.2010.11.003

[62] Zhurov, A.I.; Limbert, G.; Aeschlimann, D.P.; Middleton, J.: A constitutive model for the periodontal ligament as a compressible transversely isotropic visco-hyperelastic tissue, Computer methods in biomechanics and biomedical engineering, 10(3), 2007, 223–35. https://doi.org/10.1080/13639080701314894